

AD-A040 919

AIR FORCE GEOPHYSICS LAB HANSCOM AFB MASS
A MODEL FOR THE ELECTRICAL CURRENT COLLECTED BY A PLANAR APERTU--ETC(U)
APR 77 F J RICH, P J WILDMAN

F/G 4/1

UNCLASSIFIED

AFGL-TR-77-0096

NL

| OF |
AD
A040919



END

DATE
FILMED
4-77

ADA 040919

AFGL-TR-77-0096
ENVIRONMENTAL RESEARCH PAPERS, NO. 595



A Model for the Electrical Current Collected by a Planar Aperture Ion Collector With a Partially Blocked Field of View

FREDERICK J. RICH
PETER J.L. WILDMAN

25 April 1977



Approved for public release; distribution unlimited.

SPACE PHYSICS DIVISION PROJECT 2311
AIR FORCE GEOPHYSICS LABORATORY
HANSCOM AFB, MASSACHUSETTS 01731

AIR FORCE SYSTEMS COMMAND, USAF

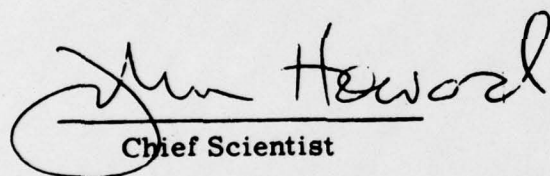


AD No. _____
DDC FILE COPY.

This report has been reviewed by the ESD Information Office (OI) and is
releasable to the National Technical Information Service (NTIS).

This technical report has been reviewed and
is approved for publication.

FOR THE COMMANDER



John Howard
Chief Scientist

Qualified requestors may obtain additional copies from the
Defense Documentation Center. All others should apply to the
National Technical Information Service.

Unclassified

SECURITY CLASSIFICATION OF THIS PAGE (When Data Entered)

DD FORM 1 JAN 73 1473 EDITION OF 1 NOV 65 IS OBSOLETE

Unclassified

Unclassified

409578

63

Unclassified

SECURITY CLASSIFICATION OF THIS PAGE (When Data Entered)

20. Abstract (Continued)

spacecraft skin. However, the model can easily be adapted to many other cases of obstructions in the field of view.

For collection of data when the ambient ion thermal speed is negligible compared to the relative bulk flow (ram) speed, the obstructions are only important when the flow vector from the ambient plasma to the plasma sensor intersects the obstructions. For the collection of data when the ion thermal speed is comparable to the relative bulk flow speed, the obstructions affect the amount of current collected by the sensors at all orientations of the spacecraft to the bulk flow direction.

Preface

This work was supported by the U.S. Air Force Geophysics Laboratory (AFGL) under Contract F19628-75-C-0081 to Regis College, Weston, MA 02193.

ACKNOWLEDGMENT	
INIS	White Section
CGC	Buff Section
CHANGING CODE	
CERTIFICATION	
DRAFT	
DISTRIBUTION/AVAILABILITY CODES	
DATA	TYPE, END, OR SPECIAL
P	

Contents

1. INTRODUCTION	7
2. INSTRUMENTATION	8
3. CALCULATION OF CURRENT TO A PARTIALLY BLOCKED PLANAR SENSOR	12
4. DISCUSSION	18
5. CONCLUSIONS	19
REFERENCES	20

Illustrations

1. Three Views of the Exterior of the Ion Bulk Motion Experiment Instrument	9
2. Orientation of Satellite With Respect to Its Orbit Path and the Earth's Surface	10
3. Field of View of Planar Sensors Looking Out of the Spin Plane	11
4. Field of View of Planar Sensors Looking In the Spin Plane	12
5. Orientation of the Two Wedges Used to Model the Obstruction for the Out-of-Plane Sensor's Field of View	13
6. Orientation of the Two Wedges Used to Model the Obstruction for the In-Plane Sensor's Field of View	13

Illustrations

7. Comparison of the Best Fit Possible With the Unobstructed Flow
Formula and the Formula Obtained Herein

20

A Model for the Electrical Current Collected by a Planar Aperture Ion Collector With a Partially Blocked Field of View

1. INTRODUCTION

Instruments designed to measure the bulk motions of environmental ions in the upper atmosphere were flown on two Air Force scientific satellites. Each instrument consisted of an array of four identical planar electrostatic analyzers. A planar electrostatic analyzer measures the flux of positive ions through an aperture from a field of view of 2π steradians. The amount of positive flux or current measured is a function of the analyzer's efficiency, its aperture area, the ambient ion density, the mean thermal speed of the ions, and the bulk flow velocity of the ions relative to the plane of the aperture. The aperture planes of the analyzers or sensors in each instrument are separated from one another by approximately 40 deg. If the mean thermal speed of the ions and the velocity of bulk plasma flow are significantly less than the satellite velocity, the difference in current flowing to the various unobstructed sensor apertures can be used to determine the spacecraft attitude.¹ Conversely, if the spacecraft attitude is known, the

(Received for publication 22 April 1977)

1. Sagalyn, R.C., and Smiddy, M. (1969) Positive ion measurements of space-craft altitude: *Gemini X and XII*, J. Spacecraft and Rockets 6(9):985-991.

instrument can be used to determine the magnitude and direction of bulk motions of the environmental ions.²

The two spacecraft, referred to here as satellites A and B, were launched into high inclination orbits with perigees of approximately 250 km. Satellite A has an apogee of 1500 km, and satellite B has an apogee of 8000 km. Both spacecraft also carry boom-mounted spherical electrostatic analyzers to determine the density and temperature of environmental electrons. Also, onboard sensors continuously determine the spacecraft attitude.

Previously developed methods to analyze the data from similar instruments have had to be significantly modified for two reasons. First, the fields of view of the individual sensors are all somewhat less than 2π steradians. This is due to a spacecraft design compromise that led to the placing of the instrument below the level of the spacecraft surface. Second, over a considerable part of both spacecraft orbits, the mean ion thermal speed cannot be taken as negligible compared to the spacecraft velocity.

This report shows the development of a procedure for analyzing the data from the ion bulk motion instruments. The current to each sensor is modelled based on the obstruction of the field of view and the fact that the ion thermal speed may be comparable to the satellite velocity. Although the development is specific, it is easily adapted to other, similar instruments.

2. INSTRUMENTATION

The basic design of the planar electrostatic analyzer in the bulk motion instruments has been given in detail elsewhere.^{2, 3, 4, 5} Below, a brief description of the instrument and its sensors is given to aid the reader in understanding the development of the modelling of the currents, which is given in Section 3.

The instrument with its four sensors is shown in Figure 1. Each sensor measures the flux of positive ions through the aperture. All the apertures have equal area. The normals of the aperture planes are set approximately 40 deg

-
2. Lai, S. T., Smiddy, M., and Wildman, P.J. L. (1976) Satellite sensing of low energy plasma bulk motion, Proc. AIAA Conf. on Aerospace and Aeronautical Meteorology and Symposium on Remote Sensing from Satellites, Melbourne, Florida, p. 302.
 3. Sagalyn, R.C., and Smiddy, M. (1967) Positive Ion Sensing System for the Measurement of Spacecraft Pitch and Yaw, Air Force D-10 Experiment Flown on Gemini X and XII, technical memorandum AFCRL-67-0158.
 4. Wildman, P.J. L. (1977) A low energy ion sensor for space measurements with reduced photo-sensitivity, to appear in Space Sci. Instrum. 3(No. 4).
 5. Wildman, P.J. L. (1976) Studies of Low Energy Plasma Motion: Results and a New Technique, AFGL-TR-76-0168.

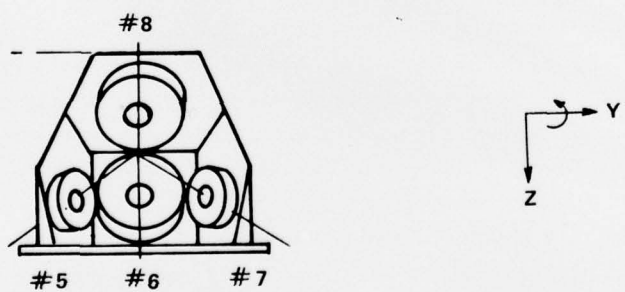
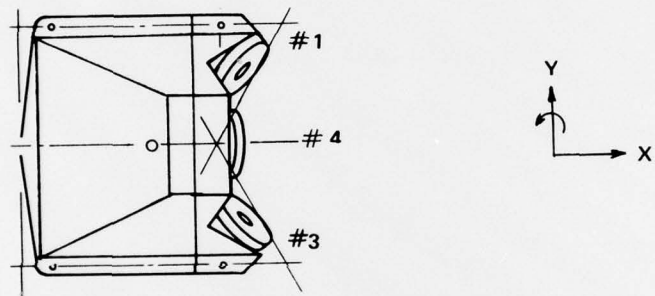
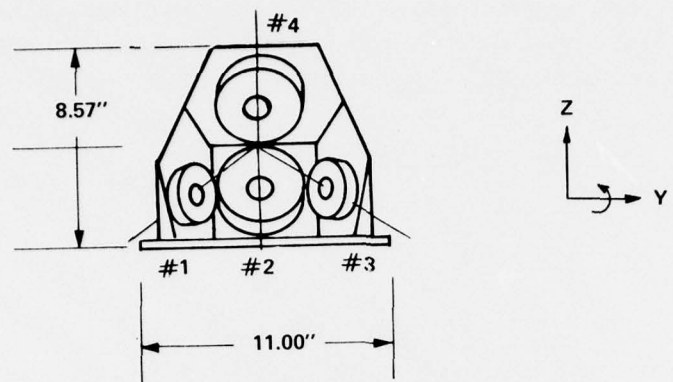


Figure 1. Three Views of the Exterior of the Ion Bulk Motion Experiment Instrument

apart from one another. Two sensors of each instrument look into the spin plane, and two sensors look out of this plane. The satellite's nominal spin axis is designated as the minus y -axis. The spin plane nominally lies in the satellite x - z plane. The $+y$ -axis is parallel to the satellite's orbital momentum vector (Figure 2).

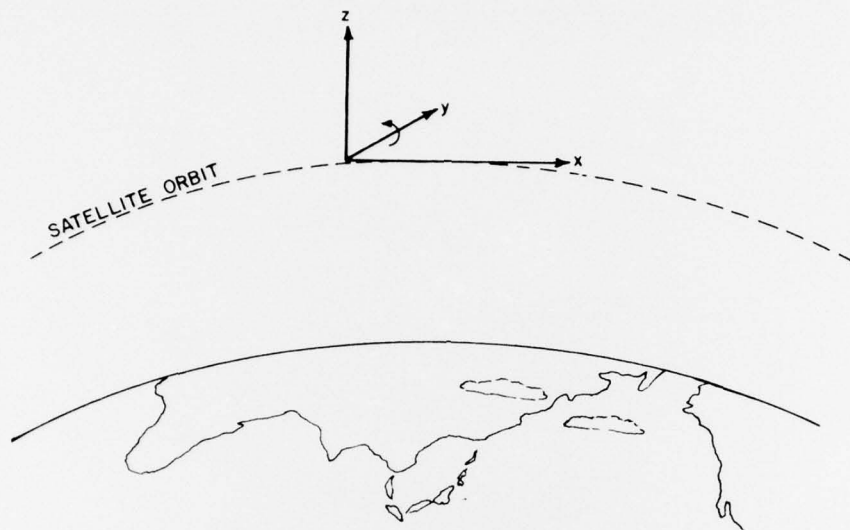


Figure 2. Orientation of Satellite With Respect to Its Orbit Path and the Earth's Surface

On satellite A, there are two instruments, one facing the $+\hat{x}$ direction of the satellite and one facing the $-\hat{x}$ direction. The four sensors in the instrument facing the $+\hat{x}$ direction are numbered as sensors 1 through 4. Numbers 2 and 4 look into the spin plane. Number 1 looks 40 deg out of the spin plane toward the $-\hat{y}$ axis, and number 3 looks 40 deg out of the spin plane toward the $+\hat{y}$ axis. The four sensors in the instrument facing the $-\hat{x}$ direction are numbered as sensors 5 through 8. The orientation of these sensors within the instrument is identical to the orientation described above for the $+\hat{x}$ facing instrument. Sensor number 5 corresponds to sensor number 1, etc. On satellite B there is only one instrument; it faces the $-\hat{x}$ direction of the satellite. The sensors are numbered 1 through 4 in the same manner as those in the instrument on satellite A.

Because the sensors in an instrument form a concave recess (Figure 1) and because the instrument itself is recessed into the satellite surface, the apertures of the sensors are below the plane of the spacecraft surface. The center of the aperture of the sensors looking into the spin plane is 48 mm below the surface, and the center of those looking out of the spin plane is 37 mm below the spacecraft surface. Thus, unlike planar sensors that are flush-mounted with a spacecraft surface, the sensors in the ion bulk motion instrument have a significant portion of their field obstructed by the spacecraft surface. Figures 3 and 4 show the fields of view for out-of-plane and in-plane sensors, respectively. For cases where the Mach number of the satellite's motion relative to the ambient plasma is large ($M \gg 1$), the current to a sensor is severely limited when the plasma flow vector intercepts a portion of the spacecraft surface before reaching the sensor aperture. When the flow vector does not intercept the surface, the current is similar to that detected by an "unobstructed" sensor. For the case when the Mach number of the satellite motion relative to the ambient plasma is near one ($M \gtrsim 1$), the current measured by a sensor is less than would be measured by an "unobstructed" sensor for all directions of the flow vector. The degree of the reduction depends upon the orientation of the obstruction to the flow direction.

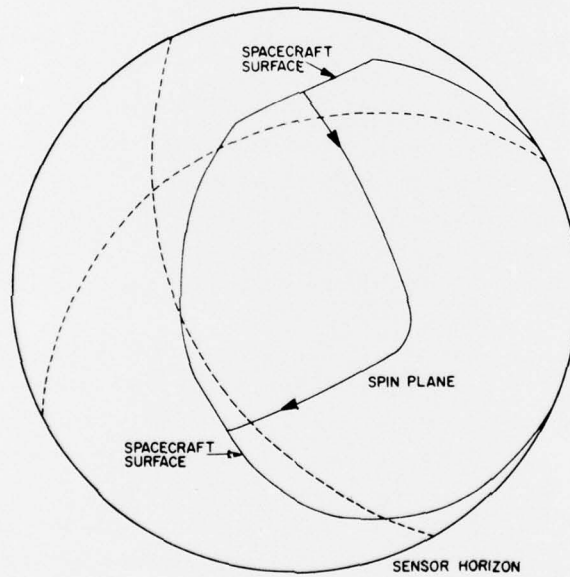


Figure 3. Field of View of Planar Sensors Looking Out of the Spin Plane

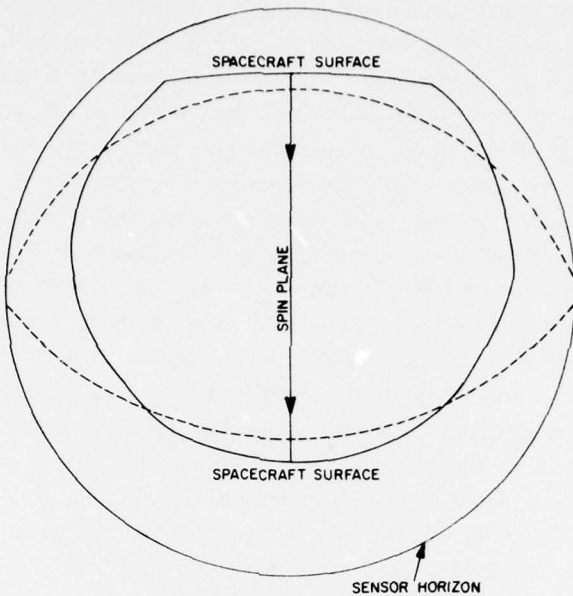


Figure 4. Field of View of Planar Sensors Looking In the Spin Plane

3. CALCULATION OF CURRENT TO A PARTIALLY BLOCKED PLANAR SENSOR

To model exactly the shape of the obstruction of flow to the sensor (Figures 3 and 4) would require an algorithm that would not be efficient for the analysis of large blocks of data. Instead, the obstructions are approximated by a series of wedges centered on the sensors' apertures. The apertures are approximated by a point located at the aperture center. Figures 5 and 6 show the arrangement of the wedges, and Figures 3 and 4 show the image of the wedges (dotted lines) in the fields of view.

The calculations are done in a sensor-centered coordinate system labeled as the $\hat{x}_s, \hat{l}_s, \hat{m}_s$ system. The \hat{x}_s axis is normal to the plane of the sensor. The \hat{l}_s axis is perpendicular to both the \hat{x}_s axis and the normal to the surface into which the instrument is mounted. The \hat{m}_s axis completes a right-handed system. For the sake of mathematical convenience, the wedges are aligned with the \hat{l}_s and \hat{m}_s axis. Thus, for the sensors that look out of the spin plane, it is necessary to make a rotation of this coordinate system to get the best alignment of the wedges with the actual obstructions. For the sensors looking below the spin plane, the above coordinate system is rotated -64 deg about the \hat{x}_s axis, and for the sensors looking above the spin plane, the rotation is -116 deg about the \hat{x}_s axis.

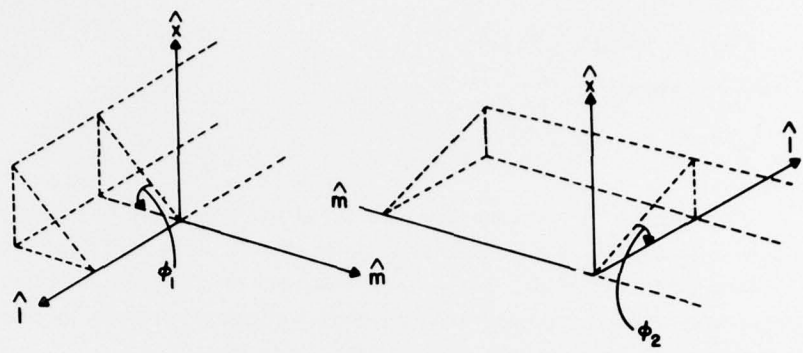


Figure 5. Orientation of the Two Wedges Used to Model the Obstruction for the Out-of-Plane Sensor's Field of View

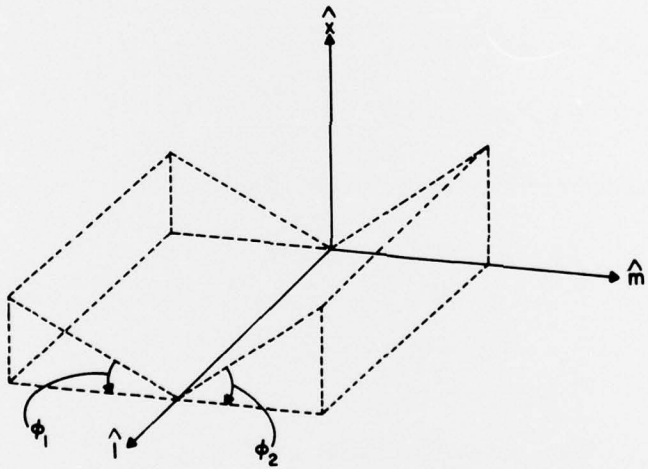


Figure 6. Orientation of the Two Wedges Used to Model the Obstruction for the In-Plane Sensor's Field of View

The expressions for the sensor's axes, in spacecraft coordinates, are:

$$\hat{x}_s = \begin{pmatrix} \cos P_s \cos Y_s \\ \sin Y_s \\ \sin P_s \cos Y_s \end{pmatrix} \quad (1)$$

where, P_s = pitch angle of the sensor's look direction measured from the $+\hat{x}$ axis of the spacecraft, and Y_s = yaw angle of the sensor's look direction measured from the spacecraft X-Y plane. Since the instrument on satellite A faces the $+\hat{x}$ direction, and since the second instrument on satellite A and the instrument on satellite B face the $-\hat{x}$ direction,

$$\hat{l}_s = (\hat{x} \times \hat{x}_s) / \text{magnitude } (\hat{x} \times \hat{x}_s) = \begin{pmatrix} 0 \\ -\sin P_s \cos Y_s / (\cos^2 Y_s \sin^2 P_s + \sin^2 Y_s)^{\frac{1}{2}} \\ \sin Y_s / (\cos^2 Y_s \sin^2 P_s + \sin^2 Y_s)^{\frac{1}{2}} \end{pmatrix} \quad (2a)$$

for sensors facing the $+\hat{x}$ direction,

$$\hat{f}_s = -(\hat{x} \times \hat{x}_s) / \text{magnitude } (\hat{x} \times \hat{x}_s) \quad (2b)$$

for sensors facing the $-\hat{x}$ direction. The third axis is:

$$\hat{m}_s = \hat{x}_s \times \hat{l}_s = \pm \begin{pmatrix} (\cos^2 Y_s \sin^2 P_s + \sin^2 Y_s)^{\frac{1}{2}} \\ -\cos Y_s \sin Y_s \cos P_s / (\cos^2 Y_s \sin^2 P_s + \sin^2 Y_s)^{\frac{1}{2}} \\ -\cos^2 Y_s \cos P_s \sin P_s / (\cos^2 Y_s \sin^2 P_s + \sin^2 Y_s)^{\frac{1}{2}} \end{pmatrix} \quad (3)$$

For the sensors looking out of the spin plane:

$$\begin{aligned} \hat{l}'_s &= \cos \alpha * \hat{l}_s + \sin \alpha * \hat{m}_s \\ \hat{m}'_s &= -\sin \alpha * \hat{l}_s + \cos \alpha * \hat{m}_s \end{aligned} \quad (4)$$

where α is either -64 deg or -116 deg.

The general formula for current flowing to a surface in a plasma is:

$$I = \int (\vec{v} \cdot d\vec{s}) N e f(\vec{v}) dv \quad (5)$$

where $d\vec{s}$ = surface element

N = number density of particles

e = electronic unit of charge

$f(\vec{v})$ = particle distribution function in velocity space.

It is assumed that the particular distribution is a Maxwellian distribution:

$$f(v_x, v_y, v_z) = (a/\pi)^{3/2} \exp \left[-a(v_x^2 + v_y^2 + v_z^2) \right]$$

where $a = m/2kT = (4/\pi c^2)$

c = average thermal speed of the particles

and v_x, v_y and v_z are the rectilinear components of the velocity of a particle in a coordinate system at rest in the gas. In order to use Eq. (5), it is necessary to transform the coordinate system to the satellite frame. The transformation is:

$$v_x = v_{xs} + q \cos \theta$$

$$v_y = v_1 + q \cos \xi \quad (6)$$

$$v_z = v_m + q \cos \eta$$

where

$$\cos \theta = \hat{x}_s \cdot (-\vec{q})/q$$

$$\cos \xi = \hat{1} \cdot (-\vec{q})/q$$

$$\cos \eta = \hat{m} \cdot (-\vec{q})/q$$

\vec{q} = velocity of the bulk flow with respect to the satellite.

The bulk flow of ions detected by the instrument is composed of two components. The velocity of the satellite measured in geographic coordinates (v_s) causes an apparent flow of the ambient plasma in the opposite direction; this is called the ram velocity. The other component is the true bulk flow of the plasma with respect

to the earth; that is the wind. The total apparent flow velocity (\vec{q}) is defined in a non-spin coordinate system such that the \hat{x} axis is parallel to the satellite velocity vector, the \hat{y} axis is perpendicular to both the satellite velocity and radius vectors, and the \hat{z} axis completes a right-handed system. In this system, the components of the wind are (DX, DY, DZ). The total apparent flow velocity can be written:

$$-\vec{q} = \vec{V}_{\text{satellite}} - \vec{V}_{\text{wind}} = \begin{pmatrix} V_s - DX \\ -DY \\ -DZ \end{pmatrix}.$$

From the onboard altitude data, the pitch and yaw of the satellite velocity is known at all times and the bulk flow velocity, expressed in satellite coordinates, is:

$$-\vec{q} = \begin{pmatrix} \cos P_v \cos Y_v (V_s - DX) + \cos P_v \sin Y_v DY + \sin P_v DZ \\ \sin Y_v (V_s - DX) - \cos Y_v DY \\ \sin P_v \cos Y_v (V_s - DX) + \sin P_v \sin Y_v DY - \cos P_v DZ \end{pmatrix}. \quad (7)$$

It is only necessary to substitute Eqs. (6) and (7) into Eq. (5) and integrate over the proper limits.

In order to maximize the speed with which the integration can be done with a digital computer, the observed current (I_s) is not computed by direct integration. Instead, the current blocked by each wedge (I_1 and I_2) is subtracted from the total current flowing to an unobstructed sensor (I_0). Note that in the case of the sensors looking out of the spin plane, the current from the region where the two wedges overlap is subtracted twice. This error is considered to be negligible, since the area of overlap is small and is always separated from the bulk flow direction by a large angle. Thus, the calculated current is:

$$I_s = I_0 - I_1 - I_2 \quad (8)$$

where

$$I_0 = 1/2 NeAq \cos \theta [1 + \text{erf}(w) + \exp(-w^2/w\sqrt{\pi})]$$

A = area of the aperture

$$w = q\sqrt{a} \cos \theta$$

For the out-of-spin-plane sensors,

$$I_1 = N e A (a/\pi)^{3/2} \int_{-\infty}^{\infty} d\nu_1 \int_{-\nu_x \cot \phi_1}^{\infty} d\nu_m \int_{-\infty}^{\infty} d\nu_x (-\nu_x) \\ \exp [-a((\nu_1 + q \cos \xi)^2 + (\nu_m + q \cos \eta)^2 + (\nu_x + q \cos \theta)^2)]$$

which integrates into

$$I_1 = 1/2 N e A (a/\pi)^{1/2} \left\{ \frac{1}{2} q \cos \theta [1 + \operatorname{erf}(w) + \operatorname{erf}(-w^2/w\sqrt{\pi})] \right. \\ \left. - (a/\pi)^{1/2} \int_0^{\infty} \nu_z \operatorname{erf} [\sqrt{a} (\nu_z \cot \phi_1 \pm \cos \eta)] \exp [-a(\nu_z - q \cos \theta)^2] d\nu_z \right\} .$$

Due to the placement of the wedges, the upper sign is used for the sensors looking below the spin plane, and the lower sign is used for the sensor looking above the spin plane. The current I_2 is calculated in a similar manner to the calculation of I_1 . The result is that the total calculated current into a sensor looking out of the spin plane is:

$$I_s = 1/2 N e A (a/\pi)^{1/2} \int_0^{\infty} \nu_z \left\{ \operatorname{erf} [\sqrt{a} (\nu_z \cot \phi_1 \pm q \cos \eta)] \right. \\ \left. + \operatorname{erf} [\sqrt{a} (\nu_z \cot \phi_2 - q \cos \xi)] \right\} \exp [-a(\nu_z - q \cos \theta)^2] d\nu_z . \quad (9)$$

For the in-plane sensors, the above process is repeated with different integration limits. The result is:

$$I_s = 1/2 N e A (a/\pi)^{1/2} \int_0^{\infty} \nu_z \left\{ \operatorname{erf} [\sqrt{a} (\nu_z \cot \phi_1 + q \cos \eta)] \right. \\ \left. + \operatorname{erf} [\sqrt{a} (\nu_z \cot \phi_2 - q \cos \xi)] \right\} \exp [-a(\nu_z - q \cos \theta)^2] d\nu_z . \quad (10)$$

The integration in Eqs. (9) and (10) cannot be done analytically, but can be calculated with good accuracy with a 10-point Gaussian quadrature.

4. DISCUSSION

With the above equations, there are five unknowns to be determined: the wind velocity components (DX, DY, and DZ), the density (N), and the mean thermal speed ($c = (4/\pi a)^{1/2}$). From any one data point, only four simultaneous currents are available from the sensor array near the ram directions. Thus, at best, a solution is obtainable for only four of the five unknowns. One of the plasma parameters must be set to a value obtained from either other data or an a priori assumption.

If a series of data points is used, it is possible, in principle, to determine all five unknown plasma parameters. However, it is not always possible to determine all five unknown parameters with an acceptable degree of uncertainty. There are reasons for this limitation to the data analysis. First, the data contains noise from several sources. The use of several consecutive data points contributes more to improving the signal to noise ratio than it does to contributing information not available from a single data point. Secondly, no method has been found for determining the plasma parameters directly from the data. The set of equations represented by (9) and (10) yields the expected data as a function of the plasma parameters instead of vice versa. The parameters are found by a search of the manifold represented by them for the "solution" that yields a minimum in the difference between the expected and the real currents. While there may be a "best" solution, there may also be a number of "good" solutions for widely separated values of the parameters. In short, the best available algorithm for finding the plasma parameters can yield false answers, especially if the relationships between the data and the parameters are not clearly stated.

In order to choose which four of the five plasma parameters should be determined from the data, it is necessary to consider the relationship between the model current and the various parameters. Changes in "DZ" tend to shift the model current curves on the time axis with minimal change in the height or the shape of the curves. Changes in "DY" tend to change the magnitude of the current in the out-of-plane sensor, without significantly changing the shape of any of the curves and with a small change in the magnitude of the current to the in-plane sensors. Changes in "N" tend to change the magnitude of all currents equally, without significantly changing the slope of the current curves. Changes in "C" tend to affect the shape of the current curves and, to a lesser degree, the magnitude of the current, without significantly changing the location of the curves on the time axis. Changes in "DX" tend to affect the shape of the current versus time curves and the magnitude of the current. Thus, changes in "N" and "C" can be interpreted as changes in "DX" and vice versa.

In practice, if no additional a priori information is available, it is best to fix the value of "DX" (to a value of zero) and then solve for the other parameters. If simultaneous data from the spherical electrostatic analyzers onboard both vehicles can give the electron density with an accuracy of ~ 10 percent, the parameter "N" can be set equal to the electron density, allowing "DX" to be solved for from the ion data. In the case where a retarding potential analyzer (RPA) is available, the "DX" is determined from the RPA data.

5. CONCLUSIONS

In this report, a formula has been developed to model the current to a planar electrostatic ion sensor with a partially blocked field of view. The use of the formula is shown in Figure 7. The data were obtained from satellite A when the Mach number of the satellite relative to the ambient plasma was approximately four. Each second of data represents approximately 19 deg rotation of the satellite about its spin axis, with the ram direction passing through the zenith of the sensor's field of view. Also shown is the current curve given by Eq. (10) and the current curve given by I_0 of Eq. (8) when $q/a \gg 1$, that is, the "cosine" formula used by Lai et al.² It is obvious that the cosine formula is a poor model for the data. The complete unobstructed sensor formula represented by I_0 of Eq. (8) will give almost identical representations for the data on the left-side and center of Figure 7, but will give a value much larger than the data on the right-side where the current decreases rapidly due to the obstruction of the field of view. As the Mach number approaches one, the difference between the current calculated by the formula for the unobstructed sensor and the formula for the obstructed sensor will become significant at all parts of the current versus time curves.

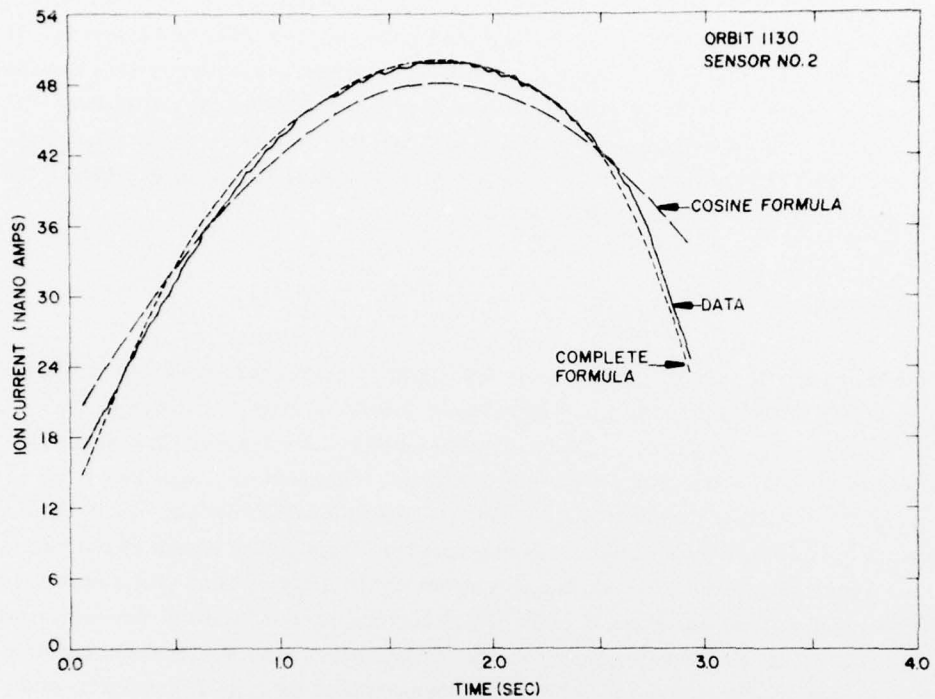


Figure 7. Comparison of the Best Fit Possible With the Unobstructed Flow Formula and the Formula Obtained Herein

References

1. Sagalyn, R.C., and Smiddy, M. (1969) Positive ion measurements of space-craft altitude: Gemini X and XII, J. Spacecraft and Rockets 6(9):985-991.
2. Lai, S.T., Smiddy, M., and Wildman, P.J.L. (1976) Satellite sensing of low energy plasma bulk motion, Proc. AIAA Conf. on Aerospace and Aeronautical Meteorology and Symposium on Remote Sensing from Satellites, Melbourne, Florida, p. 302.
3. Sagalyn, R.C., and Smiddy, M. (1967) Positive Ion Sensing System for the Measurement of Spacecraft Pitch and Yaw, Air Force D-10 Experiment Flown on Gemini X and XII, technical memorandum AFCRL-67-0158.
4. Wildman, P.J.L. (1977) A low energy ion sensor for space measurements with reduced photo-sensitivity, to appear in Space Sci. Instrum. 3(No. 4).
5. Wildman, P.J.L. (1976) Studies of Low Energy Plasma Motion: Results and a New Technique, AFGL-TR-76-0168.